

Research Article

Thermal Comfort Model Established by Using Machine Learning Strategies Based on Physiological Parameters in Hot and Cold Environments

Tseng-Fung Ho ¹, Hsin-Han Tsai ², Chi-Chih Chuang³, Dasheng Lee ², Xi-Wei Huang², Hsiang Chen ³, Chin-Chi Cheng ², Yaw-Wen Kuo⁴, Hsin-Hung Chou ⁵, Wei-Han Hsiao ⁶, Ching Hsu Yang⁷, and Yung-Hui Li ⁸

¹Department of Industrial Engineering and Management, National Chin-Yi University of Technology, No. 57, Sec. 2, Zhongshan Rd., Taiping Dist., Taichung City 411030, Taiwan

²Department of Energy and Refrigerating Air-Conditioning Engineering, National Taipei University of Technology, 1, Section 3, Zhongxiao East Road, Taipei 10608, Taiwan

³Department of Applied Materials and Optoelectronic Engineering, National Chi Nan University, Nantou 54561, Taiwan

⁴Department of Electrical Engineering, National Chi Nan University, Nantou 54561, Taiwan

⁵Department of Computer Science & Information Engineering, National Chi Nan University, Nantou 54561, Taiwan

⁶Department and Institute of Electrical Engineering, Chang Gung University, No. 259, Wenhua 1st Rd., Guishan Dist., Taoyuan City 33302, Taiwan

⁷Department of Emergency Medicine, Hsinchu Mackay Memorial Hospital, No. 690, Sec. 2, Guangfu Rd., East Dist., Hsinchu City 300041, Taiwan

⁸AI Research Center, Hon Hai Research Institute, Taipei City 114699, Taiwan

Correspondence should be addressed to Hsiang Chen; hchen@ncnu.edu.tw and Chin-Chi Cheng; newmanch@ntut.edu.tw

Received 14 March 2023; Revised 12 December 2023; Accepted 19 December 2023; Published 19 January 2024

Academic Editor: Xiaohu Yang

Copyright © 2024 Tseng-Fung Ho et al. This is an open access article distributed under the Creative Commons Attribution License, which permits unrestricted use, distribution, and reproduction in any medium, provided the original work is properly cited.

The air-conditioning systems have become an indispensable part of our daily life for keeping the quality of life. However, to improve the thermal comfort and reduce energy consumption is crucial to use the air conditioners effectively with rapid development of artificial intelligence technology. This study explored the correlation between the response of human physiological parameters and thermal sensation voting (TSV) to evaluate the comfort level among various cold and hot stimulations. The variations of the three physiological parameters, which were body surface temperature, skin blood flow (SBF), and sweat area on the skin surface, and TSV values were all positively correlated with the stimulation amount under the stimulation of cold wind, hot wind, and heat radiation, but the relationship was not completely linear. Among the three physiological parameters, the forehead skin temperature has the closest relationship with TSV, followed by the SBF and sweat. Among three stimulations, the cold wind stimulation causes the closest relationship between TSV and forehead temperature, followed by the radiation and hot wind stimulations. Through three different machine learning models, namely, random forest (RF) model, support vector machine (SVM) model, and neural network (NN) model, the stimulation of cold wind, hot wind, and heat radiation was applied to investigate the variation of the three physiological parameters as the input of the models. Moreover, the models were evaluated and verified by TSV. The results revealed that among the three different machine learning methods, RF had the best accuracy. The established thermal comfort models can predict the real-time user's thermal comfort feeling, so that air-conditioning equipment's performance can be optimized to create a healthy and energy-saving comfortable environment.

1. Introduction

According to Euromonitor statistics, the global home appliance market in 2016 was approximately US\$351 billion, especially the Asia-Pacific region accounting for 44% of the global market. Creating a comfortable environment, air-conditioning equipment has become an indispensable part of daily life. Nowadays, using air-conditioning system in an effective and energy-saving way is an important issue. To evaluate the air conditioner's (AC's) performance of comfort, the standards such as International Organization of Standardization (ISO) 7730 and American Society of Heating, Refrigerating and Air-Conditioning Engineers (ASHRAE) standard 55 [1] have been proposed. ASHRAE 55 defines thermal comfort as "the psychological state that are satisfied with the thermal environment." However, this definition only covers temperature and humidity as indicators. Incorporating factors of the occupants' objective states, the first indoor comfort model, Fanger's model [2], includes the predicted average vote (PMV) and the predicted percentage of dissatisfaction (PPD), further considering the indoor environment factors such as relative humidity, dry bulb temperature, black bulb temperature, and wind speed and human factors of activity and clothing. The model defines the human body's feeling of cold and hot in a quantitative way, laying a foundation for thermal comfort evaluation.

PMV and PPD mainly consider the comfortable level of environment objectively. However, the comfortable feelings about the dwelling environment are also related to gender, body mass index (BMI), age, activity level, and clothing [3]. Therefore, people's perception of the optimal temperature of the environment is very subjective, so it is incomplete to use temperature/humidity as a comfort index alone. There are many factors that cause human body heat loss and variation of the body surface temperature. Since the body surface is most sensitive to the environmental changes, wind speed, humidity, heat radiation, and other environmental factors can influence the amount of body heat loss. Therefore, the body surface temperature should be considered as an important human body parameter for comfort level assessment [4, 5]. When the body temperature is at a normal temperature of 37°C, the blood flow is in a stable state. However, once the temperature changes significantly, the blood flow state will also fluctuate with the temperature fluctuations. Then, the heat balance of the body may be disturbed since the blood flow transports the heat generated by cells and muscles to the whole body. To modulate the body temperature, when the ambient temperature drops, the blood vessels near the skin will shrink and the shrinkage of the blood vessels restricts the heat loss caused by the blood flow and keeps the whole body warmer. Therefore, the blood flow of the skin should be included as one of the important parameters of the human body. With the ambient temperature variation, laser Doppler radar can precisely measure the blood flow speed. When the normal temperature of the human body is 37°C, the temperature regulation mechanism of the body can keep the body in thermal balance. When the ambient temperature increases, the human body regulate the body temperature by sweat and dissipating heat to the envi-

ronment. On the contrary, in a cold environment, in order to reserve heat and keep the body warm, the body does not sweat easily. The sweat condition of the body is influenced by the ambient temperature. Therefore, sweat as one of the physiological parameters should be included so that human body thermal sensation of the subject can be accurately identified [6].

In 2007, Wang et al. [7] proposed that taking the skin temperature of the fingers, hands, and forearms may help to monitor and predict the thermal comfort state of individuals. Perceived temperatures for overall thermal comfort were collected by repeated surveys for subjects. When the ambient temperature is low, the finger temperature decreases and the blood vessels contract; when the ambient temperature is high, the finger temperature rises and the blood vessels expand since effectively providing an appropriate temperature to peripheral vascular can improve the comfort level of the human body to the environment. In 2019, Veselá et al. [8] reported that the physiological model predicts the influence of the blood flow near the skin surface caused by the skin temperature since the accuracy of the heat balance in local parts of the body may greatly affect the accuracy of the model, which contributes to effective thermal comfort adjustments in buildings. In 2020, Omidvar and Kim [9] argued that the original PMV model cannot predict accurate thermal sensation, so they modified the calculation method of heat loss from sweat evaporation in the original PMV model, thereby improving the prediction precision of the model. In the original PMV model, the sweat heat loss of low-level exercise is assumed to be zero, and the over simplification of the sweat heat loss results in structural flaws in the Fanger model. Especially in hot environments, the influence of heat loss from sweat evaporation over the entire body must be carefully considered in order to accurately evaluate the comfort level. Building a strong correlation between the environment and the human body by collecting sufficient and useful environmental and human parameters can facilitate comfort level control and create a healthy environment.

With the advancement of digital technology, incorporating artificial intelligence (AI) into the environmental comfort level control has been intensively studied. In 2016, von Grabe [10] demonstrated that the neural network (NN) method predicts thermal sensation votes on the ASHRAE thermal scale. If the interaction module between occupants and equipment in the building is provided, the energy consumption of the building can be regulated and the comfort level of the individual can be boosted. Although the thermal sensation does not represent the satisfaction of the subject with the thermal environment, it is often used as a method to evaluate the thermal comfort level. To minimize the energy consumption of buildings, it is necessary to predict the impact of interaction. von Grabe found close relationship between the gender and age of the subjects and the climatic statistics of the area as parameters with the Pearson coefficient ranging from 0.935 to 0.995 under the given conditions. In 2019, Du et al. [11] proposed that local air flow is a key factor to increase human comfort and affect air-conditioning energy consumption. Three different local air flow methods were used in his model, including isothermal

air supply, nonisothermal air supply, and floor fan. With machine learning methods, Du et al. established a database of 1305 samples, using the classification tree C5.0 model to predict 83.99% as the optimal efficiency. The result indicated that three environmental factors of temperature, air velocity, and relative humidity have dominant influence on the subjects' thermal sensation voting. The research also confirmed that machine learning is helpful for evaluating personal thermal sensation. Zhou et al. [12] applied the support vector machine (SVM) method to the thermal comfort database RP-884. They developed an AC environmental model so that natural ventilation and air-conditioning can be predicted by AI. Furthermore, by quantifying indoor air temperature, warmth with clothing, metabolic rate, and wind speed as the input variables, the model reduced the sum of squares for residuals (SSE) by 96.4% and improved the model fit by 83.7% compared with the traditional PMV model. However, the model is not favorable under extreme environmental conditions. As the reliability issues are taken into considerations, it is necessary to consider expanding the number of samples and diversity of the data to establish future models. Most of the previous studies utilized AI technology, including NN and SVM, to evaluate the personal thermal sensation via environmental factors. Some discusses its relationship with the gender, age, clothing, and metabolic rate.

The adopted keywords in the previous published papers are examined for discussing the developmental history of AI strategy applying on thermal comfort model-related research by using VOSviewer [13]. Figure 1 shows the produced scientific landscape, which is collected by coincidence of the keywords in these papers. Based on the published year, five sections, including environment, thermal sensation, prediction, local skin temperature, and building, can be identified. The most central and largest one is the environment, indicating that a suitable environment is the most important matter for human's life and the research. The thermal sensations of subjects are discussed by occupants' thermal sensation voting (TSV) or by measuring their physiological parameters of skin temperature and blood flow. SVM is often utilized to predict the skin temperature of occupant. However, the response differences of various physiological parameters under extreme stimulations, such as cold and hot air and radiation, are less investigated and evaluated. Scant research applies AI strategy on the build-up of thermal comfort model through multiple physiological parameters under extreme and combined stimulations. Therefore, this study utilizes three machine learning strategies of random forest (RF), SVM, and NN to establish thermal comfort models through multiple physiological parameters. Three stimulations, including cold and hot air and radiation, are utilized to analyze the physiological response under extreme and moderate conditions. As for the assessment of the comfort level, to achieve a people-oriented comfortable environment, the environmental parameters and human physiological parameters are collected under Taiwan's climate conditions.

2. Machine Learning Strategies

In this section, the principles and thermal comfort indexes used in the experiment are introduced. Since PMV only

evaluates the thermal comfort state of current environment objectively, three physiological parameters, including surface temperature, skin blood flow (SBF), and sweat, are taken in this study for assessing the thermal comfort state subjectively. TSV is the user's direct response to thermal changes in the environment, so the relevant physiological parameters that affect TSV are also collected to establish the more accurate thermal comfortable model.

Our previous research found that among the physiological parameters of the human body in a cold environment, the TSV model could gain the most accurate prediction and provide timeliest response by incorporating the forehead temperature, SBF, and sweat into evaluation [14]. Therefore, in this study, the same parameters of the thermal comfort parameter-based model are collected in cold and hot environments, and three machine learning strategies are used for modeling and verification.

2.1. Random Forest (RF) Model. RF model was proposed by Breiman [15]. This model adopts the concept of decision tree used for regression and classification. This machine learning algorithm is composed of a large number of decision trees with supervised learning and labeled data classifying functions, as shown in Figure 2. The RF model has advantages of fast processing, easy to use, and capable of dealing with large data sets. However, the favorable data selected by the decision trees may not be the optimal data. Especially when the tree is deeper, it is prone to overfit. Therefore, the best classification results cannot be effectively obtained when the RF contains a large number of decision trees. Still, the best solution can be approached by voting, which can compensate the problem of overfitting.

Since RF model is composed of many decision trees, information gain (IG) is an important factor in determining how to select trees from the acquired data. The factors affecting IG are Gini impurity and entropy. The higher IG is, the more complete the classification will be; the greater the Gini value is, the more chaotic the data will be; the larger the entropy is, the more irregular of the representative data sorting will be. The Gini impurity corresponds to the probability of wrong classification from selecting samples. The closer the Gini value approaches zero, the better classification will be.

2.2. Support Vector Machine (SVM) Model. SVM was proposed by Cortes and Vapnik [16] in 1995. T model belongs to supervised learning and can be used for classification and regression problems. If the input label is a continuous value, regression is performed. If the input label is discontinuous, classification is performed. The classification is mainly based on the characteristics of the samples, and the hyperplane is used to separate the samples, as shown in Figure 3. Moreover, the samples in the feature space are classified with the maximum grid distance (margin, M) as the best classification. The greater the distance between the categories is, the better the classification will be because the learning strategy is to maximize the distance between the hyperplane and the samples.

Assuming that the data set is a data set $\{x_{1,i}, x_{2,i}\}$ with n points in the set, where $i = 1, 2, \dots, n$ and x_i are real numbers,

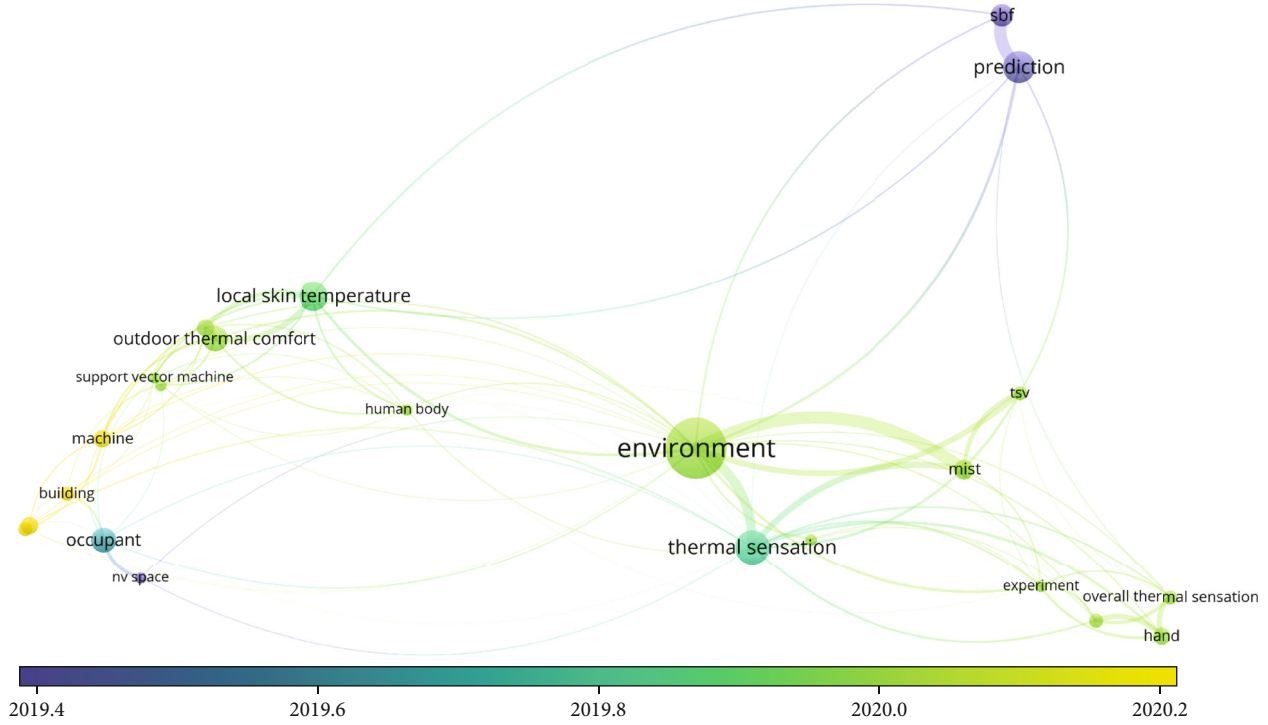


FIGURE 1: Landscape related to thermal comfort research by the publications.

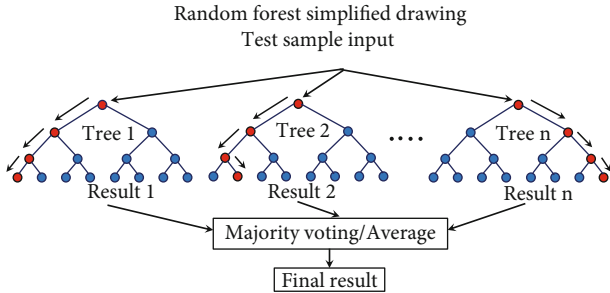


FIGURE 2: Simplified drawing of RF model, including sample input, decision trees, average of voting, and final result.

it is expected to find a linear equation to cut the data so that the data point ($y_i = +1$) is located on one side of $C1$, and the data point ($y_i = -1$) is located on the other side of the plane $C2$. The calculation process of the distance from the hyperplane is shown in the following formulas [17].

$$\begin{aligned}
 \text{Hyperplane} &= \{(x_1, x_2): w_1x_1 + w_2x_2 + b = H(x)\}, \\
 &\begin{cases} w^T x + b \geq +1 \text{ when } y_i = +1, x \in C1, \\ w^T x + b \leq -1 \text{ when } y_i = -1, x \in C2, \end{cases} \\
 M &\leq \frac{y_i H(x_i)}{\|w\|}, \quad \max_i \min_i y_i W(x_i), \\
 M\|w\| &= 1.
 \end{aligned} \tag{1}$$

2.3. *Neural Network (NN) Model.* NN was proposed by McCulloch and Walter in 1943 [18], which is a learning

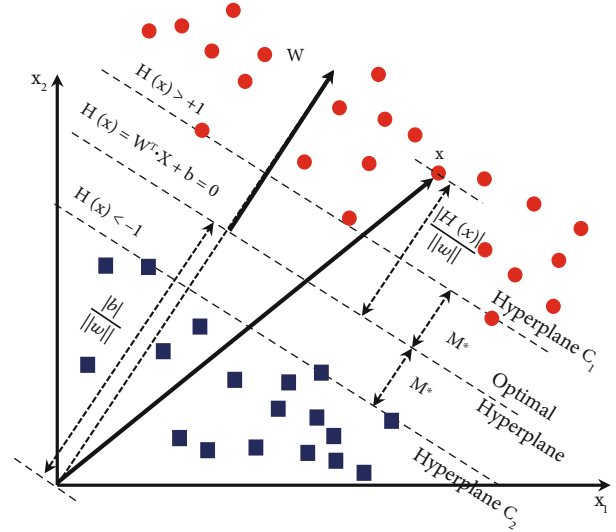


FIGURE 3: Simplified drawing of SVM model, including separating hyperplane and maximum grid distance (margin, M).

method that imitates the brain. The basic elements in the neural network are composed of many neurons (nodes) connected to each other, as shown in Figure 4. The purpose of simulating the structure of a biological neural network is to simulate the ability of the biological brain to process information. After a large number of data calculations in the input layer, hidden layer, and output layer, the NN can learn the relationship with the sample by itself.

The main feature of NN is that it can learn from past experience and can also classify disordered data through

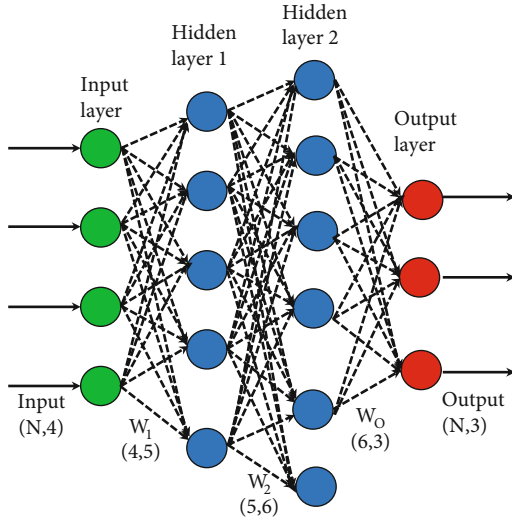


FIGURE 4: Simplified drawing of NN model, including input layer, hidden layers, and output layer.

learning. The structure of a neural network is composed of many neurons, and each layer of neurons has input between them. Between the input layer and output layer, the connection between neurons is called synapse, the weighted value on the synapse that affects the output result is called weight (w), and the activation function is introduced at the final output. If there are n input nodes (x_1, x_2, \dots, x_n), the corresponding weights are (w_1, w_2, \dots, w_n), the activation function is nonlinear, say Sigmoid function, and then, the output formula of the neuron is shown in

$$\begin{aligned} \text{Output} &= \sum (\text{input} \times \text{weight}) + \text{bias} = x_1 * w_1 + x_2 * w_2 + \dots + x_n * w_n + b, \\ z &= \sum_{i=1}^n x_i w_i + \text{bias}, \\ \sigma(z) &= \frac{1}{1 + e^{-z}}. \end{aligned} \quad (2)$$

2.4. Confusion Matrix (CM). The CM is a performance indicator for judging the machine learning classification model. The CM can be composed of binary classification or multi-class classification. It is used to measure whether the recall rate, precision, and accuracy are quite effective. The evaluation method of the confusion matrix is divided into true positive (TP), false positive (FP), true negative (TN), and false negative (FN), as shown in Figure 5. TP and TN presented as the actual and predicted results are the same, while FP and FN are the opposite. Precision is defined as the rate of data that are factually positive in all predicted positive data. Recall is defined as how many positives are correctly predicted in all positive data [19]. For samples with different characteristics, different evaluation indicators need to be selected. Precision is suitable for accurate prediction in applications, such as this establishment of the comfort model, while the actual thermal sensation voting value of the subject is the same as the judgment and prediction value of the model. Recall is suitable for detecting the presence of

		Actual values	
		Positive (1)	Negative (0)
Predicted values	Positive (1)	True positive (TP, 11)	False positive (FP, 10)
	Negative (0)	False Negative (FN, 01)	True negative (TN, 00)

FIGURE 5: Simplified drawing of CM, including four-type results of TP, FP, FN, and TN.

cancer cells in the human body. The correct prediction result is very important. The F score is also a measure of the model's accuracy and the level imbalance, calculated from the precision and recall of the CM. When $\beta = 1$, which is called $F1$ score, the precision and recall are considered equally. $F1$ score is the harmonic mean of the precision and recall. The mathematical formula definition of the evaluation index is shown in

$$\begin{aligned} \text{Precision} &= \frac{TP}{TP + FP}, \\ \text{Recall} &= \frac{TP}{TP + FN}, \\ \text{Accuracy} &= \frac{TP + TN}{TP + TN + FP + FN}, \\ F - \text{score} &= \frac{(1 + \beta^2) \text{precision} \times \text{recall}}{\beta^2 \text{precision} + \text{recall}}. \end{aligned} \quad (3)$$

3. Experiments

This research method consists of two parts. The first part is the research equipment used in the experiment, including the measuring instruments used to monitor the physiological parameters and the machine learning platform used in the subsequent establishment of the comfort model. The second part is the experimental process and conditions, including the arrangement of the experiment, the setting of the venue, and the conditions for selecting subjects.

3.1. Measuring Equipment and Machine Learning Platform. In this study, a comfort model was established including three physiological parameters of the subject's body surface temperature, SBF, and sweat volume on the skin surface, as shown in Figure 6. The equipment for measuring the three parameters is described as follows. The forehead temperature was taken by a thermocouple (SG 900, GIGARISE, Taiwan). The sensing wire was made of Teflon wire with characteristics of corrosion-resistant, acid-alkali-resistant, high-temperature, and high-pressure resistant. The surface temperature measuring piece was made of steel and copper



FIGURE 6: Measuring instruments for physiological parameters: (a) skin temperature, (b) SBF, (c) laser Doppler flowmeter, and (d) digital USB microscope for sweat.

electroplating material capable of fast response, heat resistance, and precision. The variation of the body surface temperature was observed under different cold and heat stimuli, since the body surface temperature was the basic physiological parameter of PMV and one of the important parameters for subsequent establishment of comfort model.

The SBF of fingers was measured by using laser Doppler flowmeter (LDF, moorVMS-LDF1, Moor Instruments, UK) with optical fiber of low-energy laser light as light source. To calculate the flow rate, the output was a continuous electronic signal, which was linearly related to the number of red blood cells passing through a certain cross-section. The output signal bandwidth is 3 kHz, and the time constant is 0.1 second. The sampling depth depending on the probe design and tissue characteristics was around 1 mm. The sweat volume of the palm was measured by using a digital universal serial bus (USB) microscope (EMSA, Neon, Taiwan), with magnification rates ranging from 50x to 500x. The microscope had an effective focal length of 10 mm~250 mm and eight white LED lights as auxiliary light source. The transmission interface was USB 2.0, and the auxiliary software could be used to take pictures, record videos, and store and

exchange dynamic images on the Internet. This experiment was used to measure the amount of sweat on the surface of the subjects and observe the changes in the amount of sweat when the human body received different heat and cold stimuli. Further, sweat pores could be viewed by the microscope, and subsequent image processing was performed through MATLAB.

This research used the Azure Machine Learning Studio (AMLS) machine learning platform to analyze physiological parameters and build models, including abnormal detection and classification, clustering, regression, and other methods. Data could be uploaded to the cloud system, and function blocks were used for various program combinations. The established comfort model could be uploaded to the cloud for subsequent use. The system was quite user-friendly and capable of cloud access. In this study, three machine learning strategies, including RF, SVM, and NN, were used to build and verify models.

This study has been approved by the Taipei Medical University, Institutional Review Board for Human Subject Research (TMU-IRB), and the subjects included 30 adults aged from 20 to 30 years old. The conditions excluded the

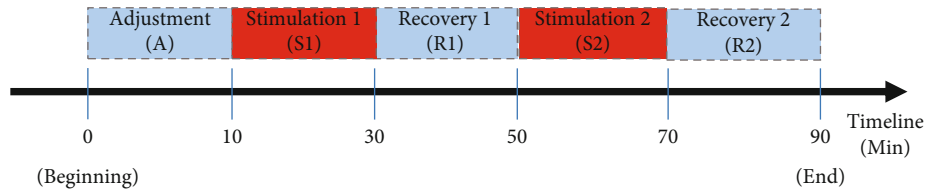


FIGURE 7: Experimental procedure and settings.

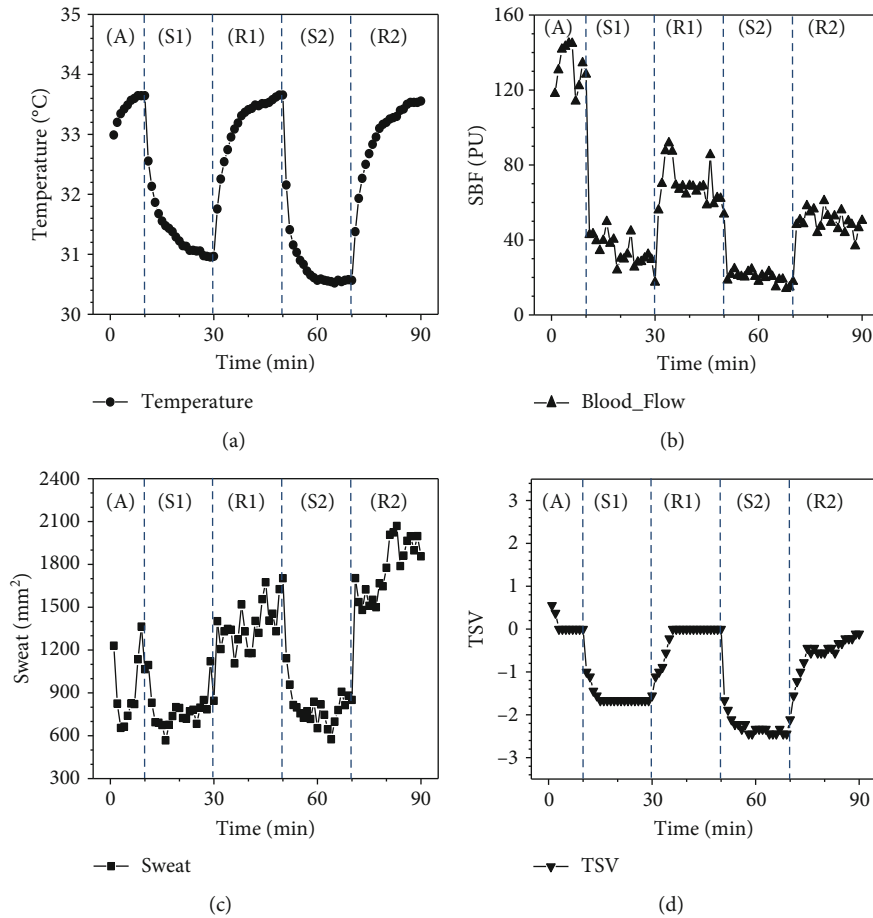


FIGURE 8: (a) Skin temperature, (b) SBF, (c) skin sweat, and (d) TSV under cold wind stimulation.

possibility of skin diseases, fever and symptoms, or the use of skin drug products known to interfere with the evaluation of skin physiology. The subjects were prohibited from strenuous exercise and drinking coffee or wine at least two days before the test, and a signed contract was required before the start of the experiment. The test subjects all agreed that the information was kept completely confidential.

3.2. Experimental Procedures and Conditions. The experimental field was in the environmental control laboratory of the Everlight Building, National Taipei University of Technology. The ambient temperature was controlled at an indoor temperature of 22°C, and the relative humidity of 60% RH was set through the Hitachi RAS-22NB split-type air conditioner. The subject was located in front of an experiment recorder, and there was a partition board between the

two to avoid possible interference. A cooling/heating fan and an electric heater were placed in front of the subject as a source of cold and heat stimulation, providing a warm and cold environment for human thermal comfort experiment.

The experimental process as shown in Figure 7 is as follows: after the subjects arrived at the experimental testing location, there was a ten-minute adjustment period to allow the subjects to adapt to the test environment, followed by a 20-minute test of stimulation 1. The conditions included three types of stimulation of cold wind stimulation (temperature 20°C, wind speed 2.42 m/s), hot wind stimulation (temperature 33°C, wind speed 0.26 m/s), and thermal radiation stimulation (temperature 25°C, wind speed 0.00 m/s) in a consecutive sequence. After that, the subjects experienced a 20-minute recovery time after the end of stimulation 1. Then, the subjects would experience a 20-minute second-

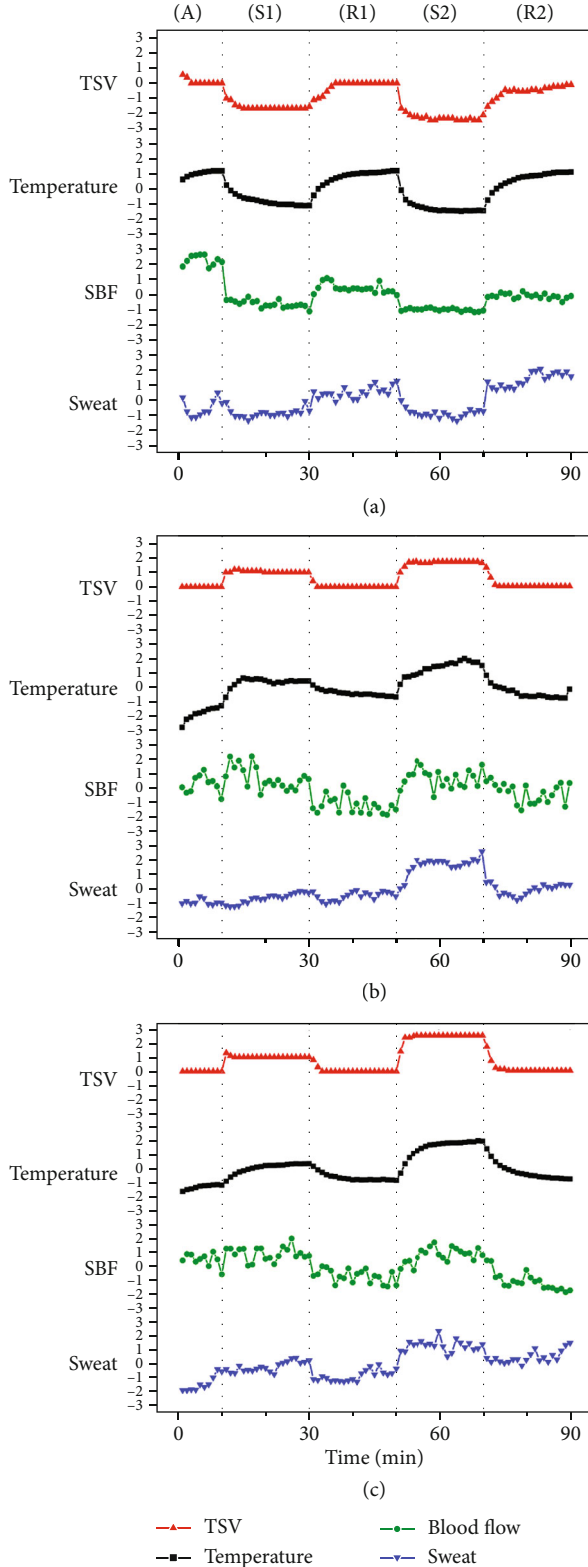


FIGURE 9: TSV and normalized physiological parameters under stimulations of (a) cold wind, (b) hot wind, and (c) radiation.

stage test of stimulation 2. The conditions were cold wind stimulation (temperature 20°C, wind speed 3.83 m/s), hot wind stimulation (temperature 40°C, wind speed 0.26 m/s),

TABLE 1: Correlation coefficient between TSV and physiological parameters under various stimulations.

Stimulation type	TSV-temperature	TSV-SBF	TSV-sweat
Cold wind	0.97	0.77	0.62
Hot wind	0.86	0.62	0.68
Radiation	0.90	0.65	0.68

TABLE 2: p values of physiological parameters between levels 1 and 2 of various stimulations.

Physiological parameters	Cold wind stimulation	Hot wind stimulation	Radiation stimulation
TSV	0.000	0.000	0.000
T	0.000	0.000	0.000
SBF	0.000	0.800	0.807
Sweat	0.685	0.000	0.000

and thermal radiation stimulation (temperature 32°C, wind speed 0.00 m/s), and there was a 20-minute recovery period after the end of the second stage. The total length of the experiment was 90 minutes.

The physiological parameters of forehead skin temperature, SBF, and sweat are measured by a surface thermometer, a laser Doppler flowmeter, and a digital USB microscope. These physiological parameters are recorded per second. During the experiment, the subjects voted for the thermal sensation of the current environment by filling out the questionnaire every minute. The thermal sensation vote was made according to the ASHRAE 55 standard [1, 20], and the thermal sensation level of the human body was divided into 7 levels of -3, -2, -1, 0, 1, 2, and 3, respectively, corresponding to whether the human body was cold, cool, slightly cool, moderate, slightly warm, warm, and hot. The evaluation of heat by voting was an important indicator of the subjects' physiological feelings about the indoor environment. The measured physiological parameters and TSV were presented in the form of the mean value and the root mean square error. In order to compare the physiological parameters with TSV, the three physiological parameters were normalized. The correlation coefficients and p values of each normalized physiological parameter between levels 1 and 2 and the four physiological parameters in each stimulation are analyzed by utilizing Pearson's method with significance level set at $p < 0.05$.

4. Results and Discussions

4.1. Physiological Parameters and TSV under Various Stimulations. In the first condition, the influence of cold wind stimulation with different wind speeds on the physiological parameters and TSV of the subjects was studied. The averaged results are shown in Figure 8.

Figure 8(a) shows the variation of forehead temperature. Based on the data collected in three time intervals of 10-30 min, 30-50 min, and 70-90 min, all the subjects' temperatures were able to return to the state at room temperature

TABLE 3: p values of physiological parameters under levels 1 and 2 of various stimulations.

Physiological parameters	Cold wind stimulation		Hot wind stimulation		Radiation stimulation	
	Level 1	Level 2	Level 1	Level 2	Level 1	Level 2
TSV_SBF	0.000	0.000	0.047	0.000	0.112	0.000
TSV_Sweat	0.000	0.000	0.000	0.847	0.000	0.000
TSV_T	0.000	0.000	0.000	0.008	0.000	0.000
T_SBF	0.041	0.003	0.196	0.001	0.000	0.000
T_Sweat	0.718	0.001	0.000	0.112	0.011	0.166
SBF_Sweat	0.0268	0.090	0.000	0.000	0.000	0.001

within a recovery period of 20 minutes. When the cold stimulus with wind speed of 2.42 m/s was introduced at 10-30 minutes, the body surface temperature dropped by 2.10°C; when the cold wind stimulus with wind speed of 3.83 m/s was introduced at 51-70 minutes, the body surface temperature dropped by 2.27°C. The degree to which the subject's body surface temperature was affected by cold wind stimulation and the temperature drop was positively correlated with the wind speed.

Moreover, Figure 8(b) shows the variation of the SBF. During the adjustment and two recovery periods, the average SBF of the subject was 132.23, 64.54, and 50.07 PU, respectively. It can be observed that the SBF cannot return close to the initial stage during the 20-minute recovery period. The short-term physiological adaptation may be the reason [21] [22]. To adjust to the variations of the environment, the human body will preserve the thermal regulation through shrinkage or expansion of blood vessels. The averaged SBF dropped from 132.23 to 34.0 and 19.79 PU under cold stimulations 1 and 2, respectively. And the averaged SBFs at recoveries 1 and 2 are 64.54 and 50.07, respectively. This information indicates that the averaged SBF decreases with the strength of cold wind stimulation.

Figure 8(c) presents the variation of the average sweat areas of the subjects. During the adjustment and two recovery periods, the average sweat areas were 1100, 1300, and 1800 mm². The drop between the initial stage and stimulation 1 and the drop between the recovery 1 and stimulation 2 were 134.69 and 486.16 mm², respectively. It can be observed that the amount of sweat of the subjects was positively correlated with the wind speed. When the cold wind stimulation was high, the subject's sweat volume decreased drastically. Figure 8(d) shows the variation of TSV. The TSV value of the subjects in the adjustment and two recovery periods returned close to 0. By contrast, in the first and second stages of cold wind stimulation, the TSV of the subjects dropped to -1.6 and -2.4. It can be seen that the degree of TSV decline was directly proportional to the intensity of cold wind stimulation. Nevertheless, because of the adjustment mechanism of the human body, the human body would gradually adapt to the temperature change of the external environment. When the external stimulation ended, the body remained in short-term thermal adaptation [22]. Therefore, the physiological values of the subject changed slowly and did not return to the initial state in time, which caused a delay. To sum up, the changes of the three physiological parameters and TSV were all related to the intensity

of cold wind stimulation, but the relationship was not completely linear.

Figure 9 shows TSV and normalized physiological parameters under stimulations of (a) cold wind, (b) hot wind, and (c) radiation. The variation of the three physiological parameters and TSV values was all positively correlated with the stimulation amount under the stimulation of hot wind and heat radiation, but the values and units between the physiological parameters and TSV values were different. For comparison, the following three physiological parameters were normalized and variation analysis was performed, as shown in Figure 9. Figure 9(a) presents the variations of four parameters when the subject was exposed to cold wind stimulation. All the three physiological parameters were obviously fluctuating and dropped with the drop of the TSV. Cold stimulation can cause the SBF at a low level owing to the contraction of the blood vessels for heat loss prevention. Furthermore, the heat loss through sweat evaporation can also be lessened because of the contraction of capillary pores. However, as the cold stimulation level increases, the sweat quantity will further decrease because of the response of cold sensors in the body. On the other hand, hot stimulation can cause the increase of the SBF level for heat dissipation because of the temperature-regulated mechanism since heat can be dissipated through sweat evaporation and SBF. The temperature-regulated mechanism of the human body can spontaneously modulate heat conservation and dissipation by adjusting various physiological parameters during cold or hot stimulation.

By contrast, Figure 9(b) shows the changes under hot wind stimulation. The three physiological parameters and TSV all changed with hot wind stimulation, but the degree of change was smaller than that of cold wind stimulation because the wind speed could counter the effect of heat generation. When stimulated, blood vessels expanded to increase SBF, and the skin temperature increased to dissipate heat to the outside ambient. Moreover, the increase of sweat on the skin surface also allowed the body to dissipate heat to the outward environment. Figure 9(c) shows the changes under thermal radiation stimulation. The three physiological parameters and TSV all changed with thermal radiation stimulation, and the degree of change was larger than that of hot wind stimulation because of the removal of the wind counter effect. The SBF and the sweat area on the skin surface were both reduced. Furthermore, the change of the sweat area in the first stage of thermal radiation stimulation was larger than that of the first stage of hot wind stimulation.

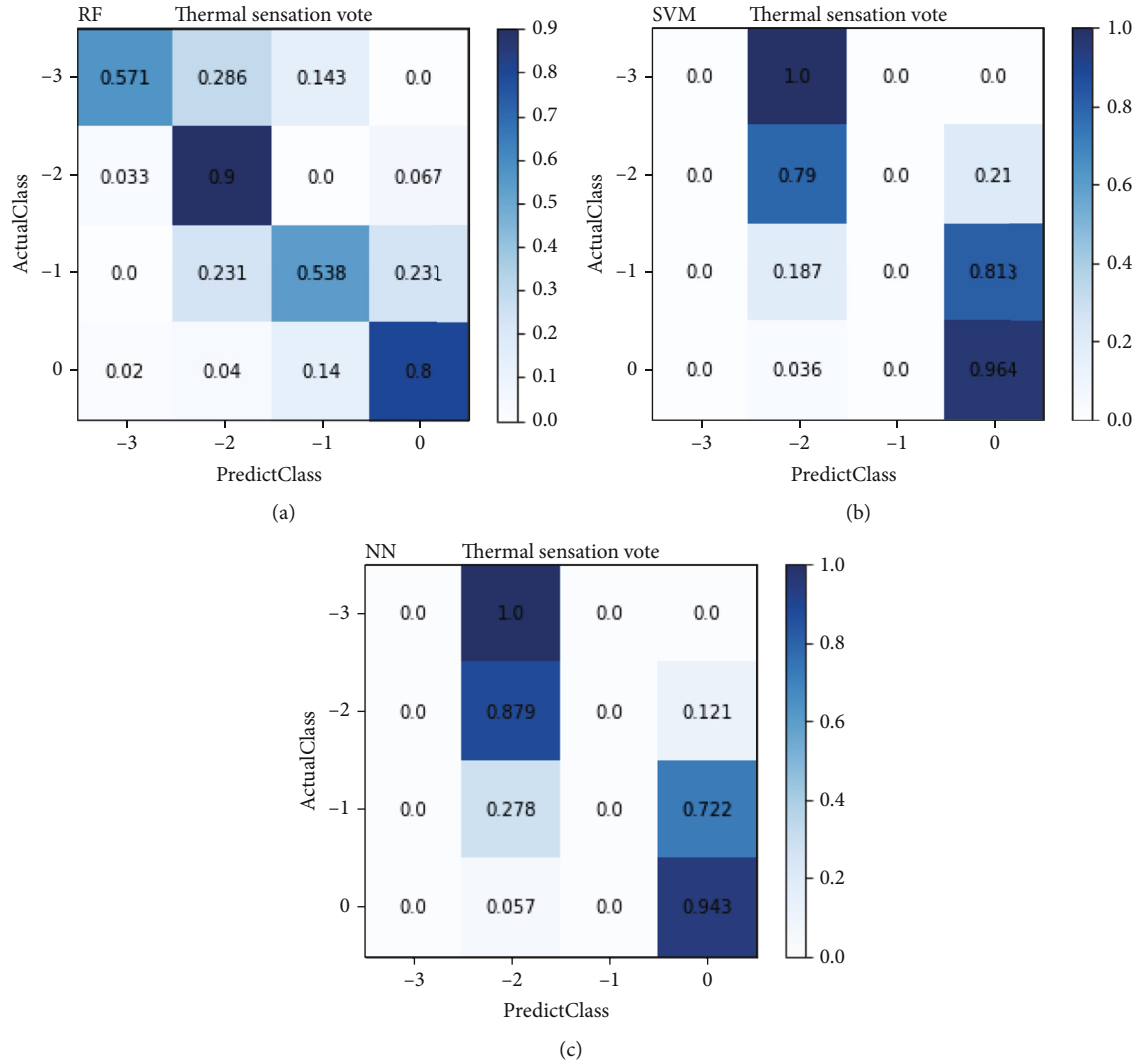


FIGURE 10: CM of thermal comfort model under cold wind stimulation established by (a) RF, (b) SVM, and (c) NN.

It can be referred that the wind mitigated the impact of heat. The correlation coefficients between TSV and normalized physiological parameters under various stimulations are presented in Table 1. Among the three physiological parameters, the forehead skin temperature has the closest relationship with TSV, followed by the SBF and sweat. Among three stimulations, the cold wind stimulation causes the closest relationship between TSV and forehead temperature, followed by the radiation and hot wind stimulations.

The p values of each normalized physiological parameter between levels 1 and 2 and the four physiological parameters in each stimulation are presented in Tables 2 and 3, respectively. In Table 2, the p value of sweat between levels 1 and 2 under cold wind stimulation is 0.68 (>0.05), indicating that the difference of sweat between levels 1 and 2 is not statistically significant. However, the p values of SBF between levels 1 and 2 under hot wind and radiation stimulations are 0.80 and 0.81, respectively. Both p values indicate that the difference of SBF between levels 1 and 2 under these two stimulations is not statistically significant. In Table 3, only the p values of TSV_temperature (T) at levels 1 and 2 of

three stimulations are less than 0.05, indicating that the differences between these two physiological parameters under the three stimulations are statistically significant. Therefore, the forehead skin temperature is the main indicator of TSV among the three stimulations. However, the p values of T_Sweat at level 1 and SBF_Sweat at level 2 of cold wind stimulation, T_SBF at level 1, TSV_Sweat and T_Sweat at level 2 of hot wind stimulation, TSV_SBF at level 1, and T_Sweat at level 2 of radiation stimulation are larger than 0.05, indicating that the differences between these two physiological parameters under the mentioned stimulations are not statistically significant. These phenomena may cause misjudge of machine learning strategies during their prediction. Even though these p values are larger than 0.05, the SBF and sweat exist the complementary action under cold and hot stimulations. This action benefits the prediction of machine learning strategies under cold and hot stimulations. The correlation coefficient results in Table 1 and p value analysis in Tables 2 and 3 describe the same tendency for the four parameters under the three stimulations.

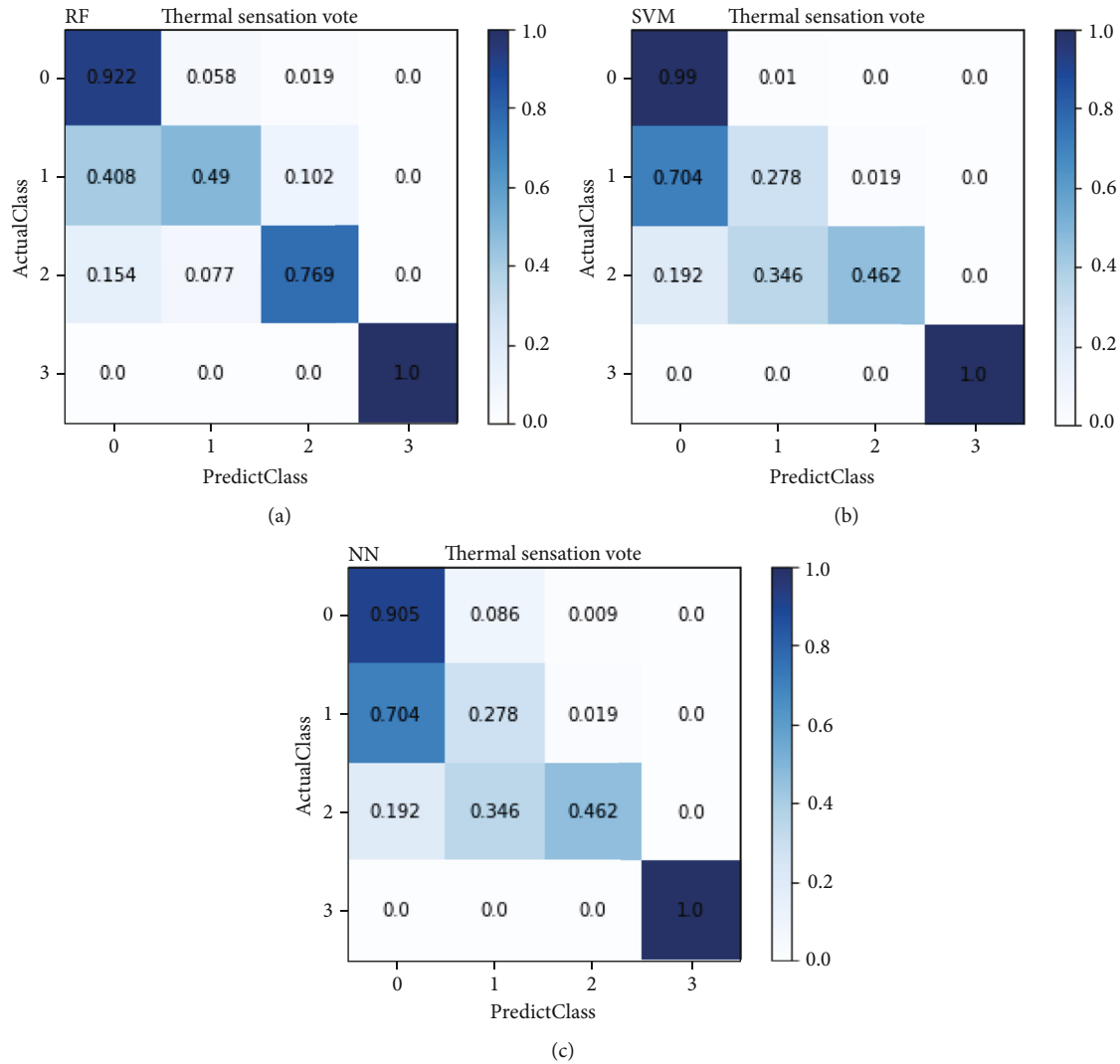


FIGURE 11: CM of thermal comfort model under hot wind stimulation established by (a) RF, (b) SVM, and (c) NN.

4.2. Thermal Comfort Model under Cold Wind Stimulation. Through three machine learning methods, namely, RF, SVM, and NN, 80% data of the subjects' responses to cold wind stimulation, hot wind stimulation, and heat radiation stimulation were used to establish a physiological parameter-based TSV model, and another 20% of the data were used to find out the best machine learning method for building the model. Finally, the performances of the established models under the combined stimulation were compared with recent related research results.

Under the stimulation of cold wind, there were four levels of TSV feedback from the subjects, 0 (moderate), -1 (slightly cool), -2 (cool), and -3 (cold), which were established through three machine learning strategies. The model presented through the CM of the prediction and actual value comparison is shown in Figure 10.

Figure 10 shows CM of thermal comfort model under cold wind stimulation established by (a) RF, (b) SVM, and (c) NN. It can be observed that in the case of TSV = -2, the accuracy predicted by RF in Figure 10(a) is more accurate than other classes and other models. According to the

analysis of physiological parameters, TSV, environmental conditions, and experimental process, the strong cold wind stimulation in the second stage caused the significant change of subjects' TSV value, which is related to the response of physiological parameters. Therefore, the accuracy of random forest classification at TSV = -2 was relatively high. At TSV = -1, because the value of physiological parameters was close to the degree of coolness, the response was relatively unclear. Further, at TSV = -3, because the responding number and period were not large and the value of the physiological parameters was close to the degree of coolness, it affected the judgment of RF in the classification. Figure 10(b) presents the model established by SVM. At TSV = 0, the accuracy predicted by SVM was relatively high, followed by TSV = -2. The prediction results of TSV = -3 and -1 were completely as cool. It can be noted that only a small number of TSV values of the subjects fallen in the cool and the slightly cool situation was predicted as moderate, since the values of physiological parameters had no obvious differences at this stage. Figure 10(c) presents the model established by NN. At TSV = 0, the prediction by NN still

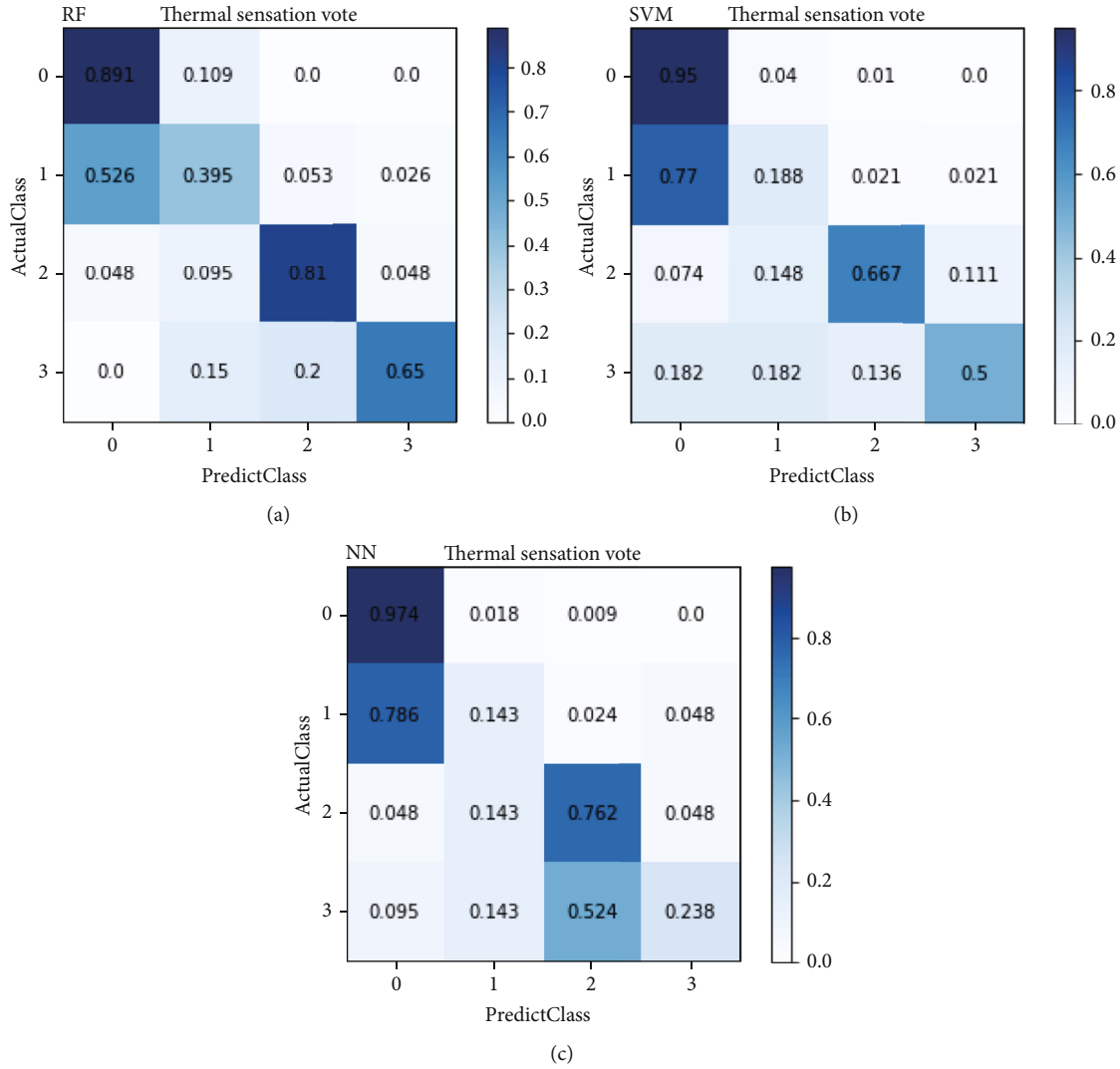


FIGURE 12: CM of thermal comfort model under radiation stimulation established by (a) RF, (b) SVM, and (c) NN.

had high accuracy. The model also had a good performance at $TSV = -2$, but there was no prediction value at $TSV = -3$ and -1 , because the physiological parameters did not differ significantly at this stage. The prediction accuracies of the three machine learning methods were 0.788 (RF), 0.67 (SVM), and 0.669 (NN), respectively. Therefore, the model established by RF was the most suitable one for cold wind stimulation.

4.3. Thermal Comfort Model under Hot Wind Stimulation. The TSV stimulated by the hot wind had four levels of 0 (moderate), 1 (slightly warm), 2 (warm), and 3 (hot) with the feedback of the subjects. Figure 11 shows CM of thermal comfort model under hot wind stimulation established by (a) RF, (b) SVM, and (c) NN. It can be observed that the accuracy predicted by RF, as shown in Figure 11(a), in the case of $TSV = 1$ was the worst case compared with other classes. The SBF and the sweat volume tended to fluctuate at TSV of 0 and 1, so it was easy to make wrong predictions during classification. By contrast, while $TSV = 2$, the physiological parameters had a clear response to external stimuli,

and the accuracy of classification was higher than the accuracy when $TSV = 1$. Moreover, when $TSV = 3$, the accuracy was the highest, because the TSV of the subjects in this case was very consistent.

In Figure 11(b) of SVM, both $TSV = 0$ and 3 had the good prediction accuracy, but $TSV = 1$ was poor in prediction. Some physiological values at class = 1 were predicted as $TSV = 2$ (0.019), because the physiological parameters did not change significantly corresponding to the subject's TSV when the subjects received external stimuli. The predicted result of $TSV = 2$ is 0.462, and part of physiological values at class = 2 fell into the predicted value at $TSV = 1$ (0.019), because the thermal sensation did not follow with the response of physiological parameters. In Figure 11(c) of NN, both $TSV = 0$ and 3 had the good prediction accuracy, but $TSV = 1$ and 2 were not good in prediction accuracy. The reason was the same as in SVM prediction. The prediction accuracies of the three machine learning strategies were 0.79 (RF), 0.667 (SVM), and 0.676 (NN), respectively. Therefore, RF was still the most suitable model for hot wind stimulation.

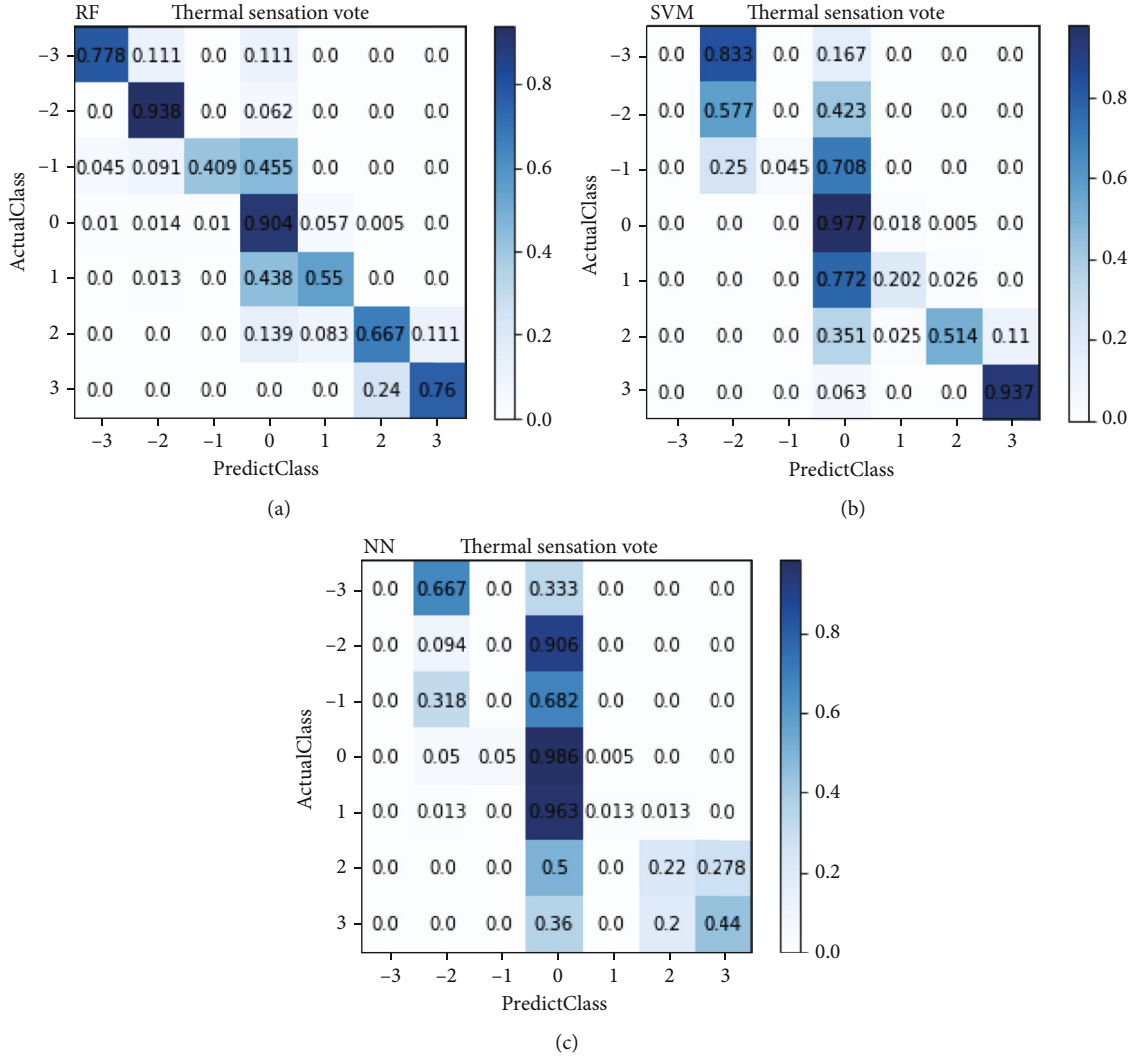


FIGURE 13: CM of thermal comfort model under combined stimulation established by (a) RF, (b) SVM, and (c) NN.

4.4. *Thermal Comfort Model under Thermal Radiation Stimulation.* The TSV stimulated by thermal radiation had four levels of 0 (moderate), 1 (slightly warm), 2 (warm), and 3 (hot) with the feedback of the subjects. Figure 12 shows CM of thermal comfort model under radiation stimulation established by (a) RF, (b) SVM, and (c) NN. In Figure 12(a) of RF model, TSV = 0 had the highest prediction accuracy, followed by TSV = 2. The prediction accuracy of TSV = 1 was the lowest of 0.395. Part of the TSV = 1 prediction was from physiological class 0 (0.109), because the stimulation from the heat radiation was relatively low at the initial stage, which made it difficult for the subjects to judge. But when the subjects received enough heat from radiation, the physiological response of the body was consistent with the thermal sensation as TSV is larger than 2. The prediction accuracy at TSV = 3 was 0.65, because the thermal radiation stimulation did not reach a very hot level. The prediction patterns of Figure 12(b) (SVM model) and Figure 12(c) (NN model) were similar to that in Figure 12(a), but the prediction accuracy was not as good as that in Figure 12(a). Therefore, SVM and NN were not good methods for establishing a

thermal comfort model. The prediction accuracies of the three machine learning strategies were 0.78 (RF), 0.763 (SVM), and 0.696 (NN), respectively. Therefore, both RF and SVM were more suitable for modeling under thermal radiation stimulation than NN.

4.5. *Thermal Comfort Model under Combined Stimulation.* The characteristics of various physiological parameters are not the same, and most of them equips nonlinear responses under cold or hot stimulations. To establish the physiological thermal comfort model under both cold and hot stimulations through linear regress may not be proper and have the high accuracy. It is our interesting to combine the TSV models under cold wind, hot wind, and radiation stimulations by machine learning strategies due to their excellent abilities for nonlinear data. Figures 13(a)–13(c) show the prediction of the cold and hot mixed stimulation based on the three machine learning strategies. The comparisons of the three models in various stimulations are shown in Tables 4 and 5.

Figure 13 shows the CM of the thermal comfort model under combined stimulation established by (a) RF, (b)

TABLE 4: Accuracies of thermal comfort models established by machine learning algorithms under various stimulations.

Stimulation type	RF	SVM	NN
Cold wind stimulation	0.788	0.67	0.669
Hot wind stimulation	0.79	0.667	0.676
Radiation stimulation	0.78	0.763	0.696
Combined stimulation	0.89	0.678	0.73

TABLE 5: *F1* score of thermal comfort models established by machine learning algorithms under combined stimulation.

Level	RF	SVM	NN
-3	0.849	Null	Null
-2	0.866	0.434	0.088
-1	0.577	0.086	Null
0	0.582	0.438	0.339
1	0.651	0.325	0.026
2	0.698	0.665	0.308
3	0.812	0.916	0.512

SVM, and (c) NN. The data indicated that the TSV = 0 state had the highest accuracy. The high accuracy was due to the fact that within the total experiment time of 90 minutes, 50 minutes was under no stimulation state. As mentioned in the previous description about model comparison in various stimulations, the predictions of the RF model were more accurate than the other two strategies. The TSV predictions in the warm and cool conditions were more accurate than that in the slightly cool and slightly warm conditions. The reason was no obvious response of physiological parameters in the initial stage of stimulation. The minor changes in physiological parameters could not stir up the human body's thermal sensation and may cause human misjudgment in TSV. Short-term thermal adaption in a change of stimulations would also cause the asynchronous phenomena between physiological parameters and TSV.

In Table 4, the thermal comfort models established by RF strategy under various stimulations present the higher accuracy than other two machine learning strategies. In Table 5, the level imbalance of thermal comfort models established by these three machine learning strategies are presented through the *F1* score. The *F1* score is also a measure of the model's accuracy, calculated from the precision and recall of the CM. The highest *F1* score appears at level 3 of SVM model. Level -3 of SVM and NN models and level -1 of NN model present lowest *F1* score, due to zero precision and recall values caused by none of the physiological and TSV data collected by these two strategies. The *F1* scores of RF model at levels -3, -2, and 3 are larger than 0.80, indicating high accuracy appearing at extreme stimulations. From levels -3 to 3, the *F1* scores of RF model are larger than other two strategies, and level differences among the various levels are less. Both results indicate the better accuracy and less level imbalance of RF model.

TABLE 6: Comparison of related research results.

Authors	Thermal comfort index	Input parameters	Algorithms (accuracy)
Wang et al. [23]	TSV	Air temperature	RF (0.77)
		Air velocity	
		CO ₂ concentration	
		Illuminance	
		Health condition	
		Living time in aged-care homes	
Liu et al. [4]	TSV	Local skin temperatures	SVM (0.92)
		Skin temperatures (head, face, abdomen, thorax, upper arm, lower arm, hand, upper leg, lower leg, feet)	
		Hand skin temperature	
		Hand skin conductance	
		Pulse rate	
		Blood oxygen saturation	
Chaudhuri et al. [24]	TSV TCV	Blood pressure	RF (0.93/0.94)
		Humidity sensation	
		Airflow sensation	
		Front head temperature	
		SBF	
		Skin sweat	
This research	TSV	RF (0.89)	SVM (0.678) NN (0.73)
		SVM (0.678)	
		NN (0.73)	

4.6. *Comparison with Related Studies.* Table 6 lists the results of other related studies. Wang et al. [23] used RF to predict the comfort level of residents in nursing homes. Six environmental variables (temperature, CO₂ concentration, air velocity, illuminance, health status, and residence time) and skin temperature of five parts (head, forearm, thigh, chest, and back) were set as the model input. Liu et al. [4] only used local skin temperatures (head, face, chest, abdomen, upper arm, lower arm, hand, thigh, calf, and foot) to establish the model by SVM. As indicated in Table 1, the skin temperature has the closest relationship with TSV. Chaudhuri et al. [24] used five physiological parameters (hand skin temperature, galvanic skin response, pulse rate, oxygen saturation level, and blood pressure) and four subjective responses (thermal comfort voting, thermal preference, humidity sensation voting, and airflow sensation voting) combined with the thermal sensation voting value. But they only discussed the model from the cold stimulation to neutral condition. In this study, the response differences of three various physiological parameters under extreme stimulations, such as cold and hot air and radiation, are investigated and evaluated. Three machine learning strategies of RF, SVM, and NN are utilized to establish thermal comfort models through three physiological parameters under extreme and combined stimulations.

4.7. *Limitations and the Future Research Outlook.* Limitations for applying these established models lie in the characteristics of subjects, types of stimulations, and the selected

artificial intelligence strategies. There are 30 young Asian students in healthy condition selected as the subjects in this study, and their ages are between 20 and 30 years old. The selected stimulations include cold wind stimulation (temperature 20°C, wind speed 2.42 m/s), hot wind stimulation (temperature 33°C, wind speed 0.26 m/s), and thermal radiation stimulation (temperature 25°C, wind speed 0.00 m/s). The selected season for test is from September to December 2019 in Taipei City, Taiwan. The selected machine learning strategies are RF, SVM, and NN for establishing thermal comfort models through three selected physiological parameters. The responses of physiological parameters and TSV of the selected subjects to the various cold wind/hot wind/radiation stimulations are discussed. Future research works will extend the study to subjects of other age levels and under various states.

5. Conclusions

In this study, the physiological parameters including forehead skin temperature, SBF, sweat on the skin surface, and thermal sensation voting value are collected through AMLS under cold wind stimulation, hot wind stimulation, and thermal radiation stimulation. The three machine learning strategies, such as RF, SVM, and NN, are used to analyze physiological parameters, establish models, and verify the thermal comfort level. As for the physiological parameter, the correlation between the forehead skin temperature and TSV is the highest, followed by SBF and sweat area. Among the three stimulations, cold wind stimulation shows the highest correlation coefficient with TSV. As for three thermal comfort models established through three machine learning strategies, when physiological parameters and TSV are used as the training data and labels, the accuracy of SVM under the combined stimulation is the lowest value of 0.678. The thermal comfort model established by RF presents the highest accuracy and less level imbalance. This information would benefit real-time prediction and control of air-conditioning equipment.

Data Availability

The data will be available based on the requirement.

Conflicts of Interest

The authors declare that they have no conflicts of interest.

Acknowledgments

This work was supported in part by the Ministry of Science and Technology, Taiwan (MOST 109-2221-E-027-012, 110-2221-E-260-006, and 111-2221-E-027-097).

References

- [1] S. C. Turner, G. Paliaga, B. M. Lynch et al., *Thermal Environmental Conditions for Human Occupancy*, Refrigerating and Air-Conditioning Engineers, Inc., American Society of Heating, 2010.
- [2] P. O. Fanger, "Calculation of thermal comfort: introduction of a basic thermo comfort equation," *ASHRAE Transactions*, vol. 73, pp. 263–271, 1967.
- [3] M. Garcia-Souto, *Temperature and comfort monitoring systems for humans*, Queen Mary, Univ London, 2012, <https://ethos.bl.uk/OrderDetails.do?uin=uk.bl.ethos.558509>.
- [4] K. Liu, T. Nie, W. Liu, Y. Liu, and D. Lai, "A machine learning approach to predict outdoor thermal comfort using local skin temperatures," *Sustainable Cities and Society*, vol. 59, article 102216, 2020.
- [5] Y. Xie, J. Niu, H. Zhang et al., "Development of a multi-nodal thermal regulation and comfort model for the outdoor environment assessment," *Building and Environment*, vol. 176, article 106809, 2020.
- [6] Y. Shimazaki and S. Katsuta, "Spatiotemporal sweat evaporation and evaporative cooling in thermal environments determined from wearable sensors," *Applied Thermal Engineering*, vol. 163, article 114422, 2019.
- [7] D. Wang, H. Zhang, E. Arens, and C. Huizenga, "Observations of upper-extremity skin temperature and corresponding overall-body thermal sensations and comfort," *Building and Environment*, vol. 42, no. 12, pp. 3933–3943, 2007.
- [8] S. Veselá, B. R. M. Kingma, A. J. H. Frijns, and W. D. van Marken Lichtenbelt, "Effect of local skin blood flow during light and medium activities on local skin temperature predictions," *Journal of Thermal Biology*, vol. 84, pp. 439–450, 2019.
- [9] A. Omidvar and J. Kim, "Modification of sweat evaporative heat loss in the PMV/PPD model to improve thermal comfort prediction in warm climates," *Building and Environment*, vol. 176, article 106868, 2020.
- [10] J. von Grabe, "Potential of artificial neural networks to predict thermal sensation votes," *Applied Energy*, vol. 161, pp. 412–424, 2016.
- [11] C. Du, B. Li, H. Liu, Y. Ji, R. Yao, and W. Yu, "Quantification of personal thermal comfort with localized airflow system based on sensitivity analysis and classification tree model," *Energy and Buildings*, vol. 194, pp. 1–1, 2019.
- [12] X. Zhou, L. Xu, J. Zhang et al., "Data-driven thermal comfort model via support vector machine algorithms: insights from ASHRAE RP-884 database," *Energy and Buildings*, vol. 211, article 109795, 2020.
- [13] J. Y. Park and Z. Nagy, "Comprehensive analysis of the relationship between thermal comfort and building control research - a data-driven literature review," *Renewable and Sustainable Energy Reviews*, vol. 82, pp. 2664–2679, 2018.
- [14] C. C. Cheng, D. Lee, and B. S. Huang, "Estimated thermal sensation models by physiological parameters during wind chill stimulation in the indoor environment," *Energy and Buildings*, vol. 172, pp. 337–348, 2018.
- [15] L. Breiman, "Random forests," *Machine Learning*, vol. 45, no. 1, pp. 5–32, 2001.
- [16] C. Cortes and V. Vapnik, "Support-vector networks," *Machine Learning*, vol. 20, no. 3, pp. 273–297, 1995.
- [17] B. E. Boser, V. N. Vapnik, and I. M. Guyon, "Training algorithm margin for optimal classifiers," in *Proceedings of the fifth annual workshop on Computational learning theory*, pp. 144–152, Pittsburgh Pennsylvania USA, July 1992.
- [18] W. S. McCulloch and P. Walter, "A logical calculus of the ideas immanent in nervous activity," *The Bulletin of Mathematical Biophysics*, vol. 5, pp. 115–133, 1943.

- [19] D. M. W. Powers, "Evaluation: from precision, recall and F-measure to ROC, informedness, markedness and correlation," 2008, <http://arxiv.org/abs/2010.16061>.
- [20] P. O. Fanger, *Thermal comfort: analysis and applications in environmental engineering*, McGraw-Hill, New York (N.Y.), 1970, <http://lib.ugent.be/catalog/rug01:000761682>.
- [21] W. Ji, B. Cao, M. Luo, and Y. Zhu, "Influence of short-term thermal experience on thermal comfort evaluations: a climate chamber experiment," *Building and Environment*, vol. 114, pp. 246–256, 2017.
- [22] C. Cheng, D. Chin, H. Tsai, and D. Lee, "Establishment of a thermal comfort model for young adults with physiological parameters in cold and hot stimulation," *Sustainability*, vol. 15, no. 3, p. 2667, 2023.
- [23] Z. Wang, H. Yu, M. Luo, Z. Wang, H. Zhang, and Y. Jiao, "Predicting older people's thermal sensation in building environment through a machine learning approach: modelling, interpretation, and application," *Building and Environment*, vol. 161, article 106231, 2019.
- [24] T. Chaudhuri, D. Zhai, Y. C. Soh, H. Li, and L. Xie, "Random forest based thermal comfort prediction from gender-specific physiological parameters using wearable sensing technology," *Energy and Buildings*, vol. 166, pp. 391–406, 2018.